Original paper

Retrospective radiological analysis of cemento-osseous dysplasia

Dilara Nil Günaçar[1,A,B,E,F], Taha Emre Köse[1,A–C,E,F], Banu Arıcıoğlu[2,D–F], Erhan Çene[3,C,F]

[1] Department of Oral and Maxillofacial Radiology, Faculty of Dentistry, Recep Tayyip Erdoğan University, Rize, Turkey
[2] Department of Endodontics, Faculty of Dentistry, Istanbul Medeniyet University, Turkey
[3] Department of Statistics, Faculty of Arts and Science, Yıldız Technical University, Istanbul, Turkey

A – research concept and design; B – collection and/or assembly of data; C – data analysis and interpretation;
D – writing the article; E – critical revision of the article; F – final approval of the article

Dental and Medical Problems, ISSN 1644-387X (print), ISSN 2300-9020 (online) *Dent Med Probl*. 2023;60(3):393–400

Address for correspondence
Taha Emre Köse
E-mail: tahaemre@gmail.com

Funding sources
None declared

Conflict of interest
None declared

Acknowledgements
None declared

Received on January 13, 2021
Reviewed on February 13, 2021
Accepted on February 16, 2021

Published online on September 30, 2023

Abstract

Background. Osseous dysplasia (OD) is a form of fibro-osseous lesion located in the jaws that may interfere with the adjacent anatomical structures.

Objectives. The aim of the present study was to evaluate the distribution of radiographic imaging features, the morphological characteristics and the lesion volume of OD with the use of cone-beam computed tomography (CBCT).

Material and methods. The study included radiologically diagnosed lesions followed up for at least 1 year. The prevalence and distribution of the OD types were defined in terms of age, sex, lesion location, teeth, relationship with the anatomical structures, and lesion volume.

Results. The mean age gradually increased from the periapical group to the florid group ($p = 0.018$). It was observed that the mandible was the most frequently affected bone (85.5%) ($p < 0.05$). The margins of the lesions were well defined, and had an irregular or circular shape. The buccal cortical bone was the most affected structure (84.5%), and the damage in the cortical bone increased with an increase in the lesion volume. With regard to teeth, the most frequent disorder was a discontinuous lamina dura (83.0%).

Conclusions. Osseous dysplasia lesions affect a wide range of different anatomical areas, and show different volume and morphometric characteristics.

Keywords: cone-beam computed tomography, bone diseases, florid cemento-osseous dysplasia

Cite as
Günaçar DN, Köse TE, Arıcıoğlu B, Çene E. Retrospective radiological analysis of cemento-osseous dysplasia. *Dent Med Probl.* 2023;60(3):393–400. doi:10.17219/dmp/133405

DOI
10.17219/dmp/133405

Introduction

Most inflammatory periapical pathologies are a consequence of dental pulp necrosis. However, other types of lesions involve hard tissue formation and are not related to the condition of the pulp.[1]

Osseous dysplasia (OD), first described by Melrose et al.,[2] is a form of fibro-osseous lesion with unknown etiology and a periapical location. In such lesions, normal bone is replaced by fibrous tissue that contains amorphous vascularized calcifications.[3] Due to its close association with the periodontal ligament and shared histopathological features, some researchers have stated that the lesion originates in the periodontal ligament, and some have suggested that the condition may arise due to the defect in extra-ligamental bone remodeling caused by local factors associated with hormonal imbalance.[4,5]

The sub-classification of OD lesions is based on their location and extent rather than the histopathological process.[6] According to localization and the extent of jaw involvement, the lesions can be classified as periapical, focal or florid OD. In periapical OD, the lower anterior teeth are usually affected. Focal OD occurs in a single area of the posterior teeth. When the lesions involve 2 or more quadrants of the jaw, it is defined as florid OD.[7] Although the term 'familial gigantiform cementoma' was used in the past as a synonym for florid OD, most authors now restrict this term to an uncommon hereditary disorder that is significantly different from the conventional OD.

Florid OD is a gnathic bone disorder that ultimately leads to the formation of substantial sclerotic masses of disorganized mineralized material, and it is typically multi-focused on both the maxilla and the mandible.[8] Radiographically, it initially occurs as multiple radiolucencies in the periapical regions, but it later develops a mixed radiolucent and radiopaque model in the affected areas. Upon further maturation, the lesions become predominantly radiopaque, but often have a thin radiolucent margin.[9]

The radiographic appearance of all forms of OD can vary from hypodense, through mixed, to hyperdense areas due to lesion maturation over time and the accumulation of mineralized tissue. Initially, the radiolucent stage may be misdiagnosed as radicular cysts or periapical granulomas because of a periapical location. However, OD is usually associated with vital teeth, presents with no clinical complaints and requires no intervention. On the other hand, OD can be observed as mixed images, with residual cysts in edentulous areas, or as mixed/radiopaque images, with increasing density and calcification in later stages and lesion maturation over time. In this phase, it is vital to differentiate between osteomas, odontogenic tumors and idiopathic osteosclerosis.[10]

Although the lesions are usually well defined, their borders tend to be slightly irregular.[11] The lesions can sometimes be confused with other single or multiple lesions that are round or oblong, defined as bone islands or enostoses.[12] Idiopathic osteosclerosis is a localized radiopaque area of unknown etiology, also called a dense bone island or enostosis. It can be well circumscribed, usually round or oval, and sometimes irregularly shaped. It is distinguished from stage 3 OD based on not having a thin radiolucent edge.[13]

Panoramic and intraoral radiographs enable a limited examination of the adjacent anatomical structures. Cone-beam computed tomography (CBCT) allows a three-dimensional (3D) evaluation of anatomical structures with minimal distortion and high spatial resolution.[14] Thus, it has been quite beneficial for the detection of OD[15]; however, as the periapical form of OD has limited size and effects on the adjacent structures, CBCT may not be required to evaluate these lesions.

In previous studies, the lesion features and the effects of OD on anatomical structures were analyzed for the first time with the use of CBCT images to measure the lesion dimensions linearly in a Brazilian population.[3] The present study aimed to evaluate the radiomorphometric characteristics of cemento-osseous lesions in a Turkish population.

Material and methods

The ethics committee at the Faculty of Medicine of the Recep Tayyip Erdoğan University, Rize, Turkey, approved this research (reference number 2020/189), which complied with the Declaration of Helsinki.

The study included the data of patients who had reported to the Department of Oral and Maxillofacial Radiology, Faculty of Dentistry, Recep Tayyip Erdoğan University, Rize, Turkey, for various reasons and had been diagnosed with cemento-osseous lesions between 2017 and 2020. All patients signed an informed consent form. The study included radiologically diagnosed lesions followed up for at least 1 year. According to the radiographic follow-up, no patient required a biopsy. For stage 1 lesions, the vitality test results from the patient files were used to differentiate OD lesions from the endodontic ones. Thus, no histopathological data was obtained.

The lesions were divided into periapical, focal or florid OD, according to anatomical locations, clinical characteristics and radiographic features.[16] Lesions located only at the anterior teeth were classified as periapical, while those on a single posterior tooth were classified as focal, and those within 2 or more quadrants were classified as florid.

The exclusion criteria were as follows: a surgical intervention at the relevant areas; a history or the presence of orthodontic treatment; infected OD lesions; and CBCT data that did not include all the OD lesion areas.

All CBCT images were obtained using a Planmeca ProMax 3D Classic unit (Planmeca, Helsinki, Finland) with the following parameters: 90 kVp; 4–10 mA; and 200 μm

voxel size. The linear measurements were taken and the lesion characteristics were assessed using the Planmeca Romexis software, v. 4.6.2.R. The 3D reconstruction and the volume measurements were conducted using InVesalius, v. 3.1.0 (Centro de Tecnologia da Informação Renato Archer, Campinas, Brazil), and free open-source software (Fig. 1). The CBCT images were assessed in relation to the multiplanar reconstruction and the cross-sectional images, based on a study by De Oliveira Kato et al.[3]

Two oral and maxillofacial radiologists with over 10 and 6 years of experience, respectively, assessed the images independently. A random selection of 20% of the CBCT scans included in the study was reassessed after 2 weeks to evaluate intra-observer reliability. The kappa coefficients were 0.83 and 0.84 for observer 1 and observer 2, respectively, which indicates excellent intra-observer reliability. Inter-observer reliability demonstrated excellent agreement, with a kappa coefficient of 0.87.[17]

The details of the patients' age and sex, the associated lesions, the lesion location (right, left, anterior, and posterior), and the total number of locations were recorded. Lesion staging was based on the presence or absence of radiopaque calcifications in the lesion area. If there was none, the lesion was classified as stage 1, if a small calcified area that did not fill all of the lesion was present, it was classified as stage 2, and if the calcified area filled all of the cavity, with or without a slim radiolucent peripheral band, it was classified as stage 3. If the lesions were associated with the teeth, the tooth numbers were recorded. The periphery of the lesion was described as either well-defined (corticated, sclerotic, non-corticated, and partially corticated) or ill-defined (perforating, diffuse and invasive). The lesion shape was recorded as circular, oval or irregular. Hypodense capsules were assessed as present, absent or partially present. Involvement with the adjacent structures, such as the cortical bone (lingual and buccal), the mandibular canal, the mental foramen, the nasopalatinal canal, the incisive foramen, the maxillary sinus, the nasal fossa, and the anterior mandibular canal, was assessed and recorded. The effects on the cortical bone were assessed as follows: intact; thinning; expansion and thinning; thinning and perforation; expansion, thinning and perforation. The internal calcified parts of the lesion and the total lesion volume were also assessed.

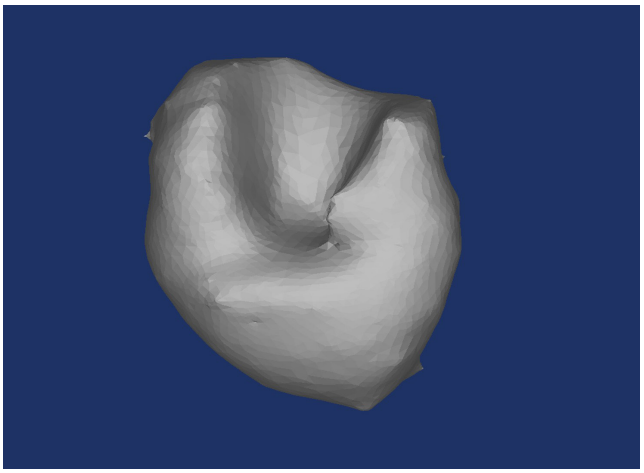

Fig. 1. Three-dimensional (3D) reconstruction of a cemento-osseous lesion

The greatest linear dimensions of the mesiodistal and buccolingual positions were measured on the axial plane, while the superoinferior dimension was measured on the cross-sectional images.

All the teeth associated with the OD lesion areas were recorded and assessed for the loss of lamina dura or periodontal ligament space, root resorption, tooth displacement, radiopacity adherent to the root, and endodontic treatment.

Statistical analysis

The IBM SPSS Statistics for Windows software, v. 23.0 (IBM Corp., Armonk, USA), was used to analyze the relationships between the different types of OD and the demographic and radiological data.

The distribution of the OD lesion types was determined using descriptive statistics and percentages. Additionally, differences in the width and depth of the lesions, according to the types and regions, were examined with the one-way analysis of variance (ANOVA) and the *t* test ($p < 0.05$). If a difference was noted, the Bonferroni test was used for multiple comparisons.

The study sample size was determined by conducting a power analysis, using G*Power (3.1.1).[18] The required sample size to reach a power of 0.90 with a type-one error (α) of 0.05 and a low effect size of 0.40 was calculated as 84.

Results

A total of 84 OD lesion areas were detected in 46 patients, including 5 males and 41 females. Female patients were more affected than male patients for all types of OD ($p < 0.05$).

The most frequent OD type was florid ($n = 17$; 37%), followed by focal ($n = 16$; 35%) and periapical ($n = 13$; 28%). Although the mean age was similar for all types of OD, it gradually increased from the periapical group to the florid group, and a statistically significant difference in the average age was observed between the periapical and florid groups ($p = 0.018$). In the periapical group, the mean age was 36.23 ±8.97 years (min: 24 years, max: 47 years), in the focal group, the mean age was 40.31 ±13.40 years (min: 21 years, max: 58 years), and in the florid group, the mean age was 47.53 ±8.46 years (min: 34 years, max: 68 years).

Irrespective of the OD type, the mandible (85.5%) was more involved than the maxilla (14.5%). The relationship between the total volume of the OD lesion areas and the cortical bone involvement is shown in Table 1.

Figure 2 shows the teeth associated with all groups. Taking into account all groups, the most frequently affected teeth were observed in the anterior region (66.0%).

When evaluating the groups separately, the buccal cortical bone (n = 15) and, in rare cases, the anterior mandibular canal (n = 4) were mostly affected by OD in the periapical group (Table 2). The affected anterior teeth often showed a discontinuous lamina dura, and an enlarged and non-uniformly visible periodontal ligament space. Hyperdense lesion areas adherent to tooth roots were observed in 2 cases (7.7%). Root resorption was not detected in any case, and tooth replacement was found only in 1 case (3.8%) (Table 3).

In the focal group, OD mostly affected the buccal (n = 13) and lingual (n = 9) cortical bone, followed by the mandibular canal (n = 6). The association with the mental foramen was detected in 2 cases and a maxillary sinus

Table 1. Changes in the cortical bone depending on the total volume of the osseous dysplasia (OD) lesion areas (Kruskal–Wallis test)

Effect on the cortical bone	*n*	Total volume of the OD lesion areas [mm^3]				*p*-value
		M ±*SD*	*Me*	min	max	
Intact	8	492.18 ±488.59	283.53	61.96	1,265.19	>0.05
Thinning	39	772.25 ±787.11	506.21	46.02	2,653.00	
Expansion and thinning	19	643.83 ±967.56	255.41	81.54	2,922.25	
Thinning and perforation	4	601.35 ±642.68	601.35	146.90	1,055.79	
Expansion, thinning and perforation	14	1,088.31 ±1,086.39	516.44	146.60	2,732.67	

M – mean; *SD* – standard deviation; *Me* – median; min – minimum; max – maximum.

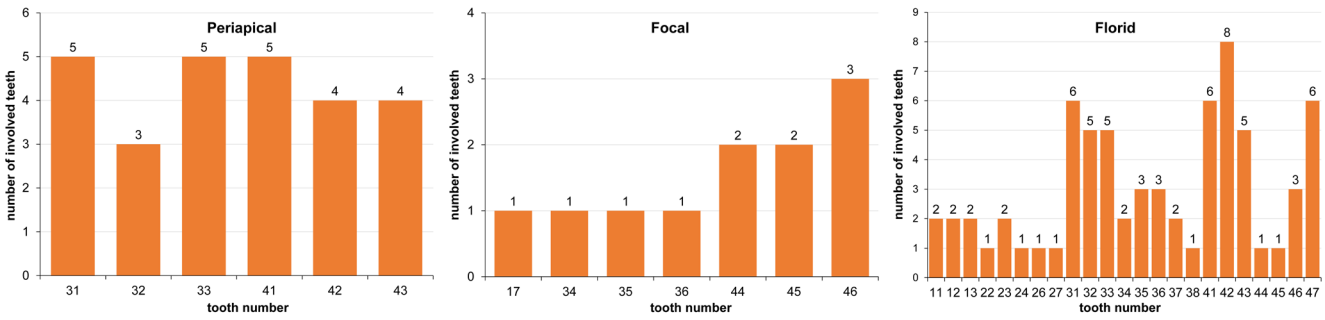

Fig. 2. Relationships between all types of osseous dysplasia (OD) lesions and the tooth numbers

Table 2. Distribution of the anatomical structures affected by periapical, focal and florid osseous dysplasia (OD)

Type of OD lesion	Anatomical structure	Mesiodistal dimension [mm]				Buccolingual/palatal dimension [mm]				Superoinferior dimension [mm]			
		n	*Me*	min	max	*n*	*Me*	min	max	*n*	*Me*	min	max
Periapical (n = 16)	cortical bone – lingual	13	7.40	3.79	18.84	13	6.40	4.02	8.25	13	7.60	2.80	11.21
	cortical bone – buccal	15	6.93	3.20	18.84	15	6.21	3.20	8.25	15	6.40	2.80	11.21
	anterior mandibular canal	4	9.38	6.93	18.84	4	6.73	6.21	6.83	4	7.60	6.40	10.22
Focal (n = 16)	cortical bone – lingual	9	8.02	5.00	15.01	9	7.06	4.57	9.65	9	7.40	5.40	10.00
	cortical bone – buccal	13	8.02	5.00	15.01	13	7.06	4.43	11.61	13	7.10	5.00	10.00
	mandibular canal	6	8.86	5.56	15.01	6	7.48	4.57	9.65	6	7.17	5.40	10.00
	mental foramen	2	6.79	5.56	8.02	2	4.84	4.57	5.11	2	5.86	5.40	6.32
	maxillary sinus	1	14.24	14.24	14.24	1	11.61	11.61	11.61	1	9.40	9.40	9.40
Florid (n = 52)	cortical bone – lingual	35	10.41	3.00	34.60	35	7.60	3.20	15.20	35	8.61	4.20	16.00
	cortical bone – buccal	43	8.60	3.20	34.60	43	7.21	2.40	15.20	43	8.20	2.83	16.00
	mandibular canal	13	10.41	4.00	19.40	13	8.21	3.62	14.04	13	12.00	6.60	13.60
	incisive foramen	2	8.10	5.80	10.40	2	5.54	3.80	7.28	2	7.34	5.00	9.67
	maxillary sinus	1	12.11	12.11	12.11	1	8.32	8.32	8.32	1	5.00	5.00	5.00
	nasal fossa	2	13.96	13.80	14.12	2	11.80	8.40	15.20	2	11.31	10.42	12.20
	anterior mandibular canal	1	5.66	5.66	5.66	1	6.40	6.40	6.40	1	4.80	4.80	4.80

relationship was detected in 1 case (Table 2). In the lesion areas, a well-defined periphery (n = 16; 100%), a partially corticated border (n = 7; 43.8%), a circular shape (n = 7; 43.8%), mixed density (n = 12; 75.0%), and a hypodense rim (n = 10; 62.5%) were detected (Table 4). The most frequently affected teeth were observed in the posterior region, especially on the right side (72.7%). While a discontinuous lamina dura and a change in periodontal ligament space were detected in 8 teeth (72.7%) in the lesion areas, no cases of root resorption or tooth displacement were found. In 2 cases, radiopaque masses adhered to the root (Table 3).

Table 3. Distribution of tooth alterations and the affected periodontal structures with regard to periapical, focal and florid osseous dysplasia (OD)

Variables	Periapical OD (n = 26)	Focal OD (n = 11)	Florid OD (n = 69)	Total (n = 106)
Lamina dura	24 (92.3)	5 (45.5)	59 (85.5)	88 (83.0)
Periodontal ligament space	21 (80.8)	3 (27.3)	47 (68.1)	71 (67.0)
Root resorption	0 (0)	0 (0)	1 (1.4)	1 (0.9)
Tooth displacement	1 (3.8)	0 (0)	5 (7.2)	6 (5.7)
Radiopacity adherent to the root	2 (7.7)	2 (18.1)	23 (33.3)	27 (25.5)
Endodontic treatment	0 (0)	0 (0)	2 (2.9)	2 (1.9)

Data presented as number (percentage) (n (%)).

The buccal (n = 43) and lingual cortical bone (n = 35) were mostly affected by lesions in the florid group. Moreover, displacement or perforation involved the mandibular canal in 13 cases, and the incisive foramen and the nasal fossa in 2 cases. In addition, the floor of the maxillary sinus (n = 1) and the anterior mandibular canal (n = 1) were related to displacement (Table 2). Most of the lesion areas demonstrated a well-defined periphery (n = 46; 88.5%), a partially corticated border (n = 20; 43.5%), an irregular shape (n = 22; 42.3%), mixed density (n = 28, 53.8%), and a hypodense rim (n = 39; 75.0%) (Table 4). The majority of lesions were found in 2 different areas (n = 8), with 5 observed in 3 different areas, 1 observed in 4, 1 observed in 5, and 2 extended to 6 different areas. The most frequently affected teeth were observed in the anterior of the mandible (50.7%), and 27.5% were on the right side. Most of the teeth affected by OD had a discontinuous lamina dura, and an enlarged and non-uniformly visible periodontal ligament space in the lesion area. Twenty-three teeth (33.3%) had hyperdense lesions adherent to tooth roots, while tooth displacement associated with OD was uncommon (Table 3).

Regarding age-related changes in radiographic features, radiolucent density was noted at the early stage of the lesion in the middle-age group (37.6 ±7.0 years), while in the 41.5 ±9.5 years age group, a mixed lesion stage was noticeable. In the group above the middle age (50.2 ±10.5 years), radiopaque masses with calcification were observed. In all types of OD, the volume of the OD lesion area was related to age, but the difference was not statistically significant (p = 0.056)

Table 4. Radiographic features of the lesion areas of periapical, focal and florid osseous dysplasia (OD)

Radiographic features		Groups			Total (N = 84)
		periapical (n = 16)	focal (n = 16)	florid (n = 52)	
Periphery	well-defined	15 (93.8)	16 (100)	46 (88.5)	77 (91.7)
	ill-defined	1 (6.3)	0 (0)	6 (11.5)	7 (8.3)
Well-defined	corticated	5 (33.3)	3 (18.8)	13 (28.3)	21 (27.3)
	sclerotic	0 (0)	2 (12.5)	4 (8.7)	6 (7.8)
	non-corticated	3 (20.0)	4 (25.0)	9 (19.6)	16 (20.8)
	partially corticated	7 (46.7)	7 (43.8)	20 (43.5)	34 (44.2)
Ill-defined	perforating	0 (0)	0 (0)	0 (0)	0 (0)
	diffuse	1 (100)	0 (0)	5 (83.3)	6 (85.7)
	invasive	0 (0)	0 (0)	1 (16.7)	1 (14.3)
Shape	circular	8 (50.0)	7 (43.8)	15 (28.8)	30 (35.7)
	oval	5 (31.3)	3 (18.8)	15 (28.8)	23 (27.4)
	irregular	3 (18.8)	6 (37.5)	22 (42.3)	31 (36.9)
Internal density	hypodense	5 (31.3)	0 (0)	6 (11.5)	11 (13.1)
	hyperdense	2 (12.5)	4 (25.0)	18 (34.6)	24 (28.6)
	mixed	9 (56.3)	12 (75.0)	28 (53.8)	49 (58.3)
Hypodense rim	present	14 (87.5)	10 (62.5)	39 (75.0)	63 (75.0)
	absent	1 (6.3)	1 (6.3)	3 (5.8)	5 (6.0)
	partially present	1 (6.3)	5 (31.3)	10 (19.2)	16 (19.0)

In all types of OD, the lesion area in each of the 3 dimensions showed no significant differences ($p > 0.05$). In the case of lesions located in the anterior and posterior regions, the mesiodistal distance was not significantly different. However, the posterior lesions showed a larger width for the buccolingual distance (7.40 ±2.74 mm) as compared to the anterior lesions (5.86 ±2.04 mm) ($p < 0.01$).

Discussion

Osseous dysplasia lesions may lead to endodontic misdiagnosis.[19] The disease is typically asymptomatic, and is usually detected when radiographs are recorded for other purposes. Correct diagnosis can pose problems, but it is crucial for proper management.[20] In most instances of OD, the distinctive clinical and radiographic patterns allow a strong presumptive diagnosis without the necessity of performing a biopsy.[21]

Periapical OD primarily involves the periapical region of the anterior mandible. The early stage of the lesion appears as a limited radiolucent area covering the apical region of the tooth. Solitary lesions may occur, but multiple foci are encountered more often.[22]

Focal OD can occur in any area of the jaw, but the posterior side of the mandible is the most affected region. Radiographically, the lesion varies from completely radiolucent to densely radiopaque with a thin radiolucent peripheral rim. However, a mixed radiolucent and radiopaque pattern is most commonly found.[23]

Florid OD presents with multifocal involvement and is not limited to the anterior mandible. Although many cases demonstrate multifocal lesions only in the posterior portions of the jaw, there are a lot of patients who also exhibit anterior mandible involvement.[6] The lesions demonstrate a marked tendency for bilateral and often quite symmetrical involvement, and it is not unusual to encounter extensive lesions in all 4 posterior quadrants.[24] Initially, the lesions are predominantly radiolucent. However, they become mixed over time and predominantly radiopaque with only a thin radiolucent peripheral rim. Occasionally, the lesion can become almost completely radiopaque and blend with the adjacent normal-appearing bone.[25]

Extensive knowledge about the characteristics of OD, correct diagnosis and the interpretation of CBCT images are crucial to avoid incorrect treatment. Therefore, this study described the demographic and general radiographic features of OD in a Turkish population, using the volume measurement and 3D technology, and compared them with the data in the existing literature. To our knowledge, this is the first study to describe the size of OD by volume with the use of CBCT.

Based on the findings of the present retrospective study, the tendency for females to exhibit OD lesions appears to be higher as compared to males. This finding is compatible with other reports in the existing literature.[15,26] In previous studies, the lesions were more common in black women in the 5th and 6th decades, and it was suggested that genetic and/or hormonal factors may be causative.[26]

Osseous dysplasia is usually detected by routine diagnostic radiographs. However, advanced imaging methods are needed to evaluate some differences in the focal and florid OD variants, and to reveal the relationships between the lesions and anatomical structures.[27] In previous reports, almost 90% of OD lesions affected the mandible and they usually occurred adjacent to the lower teeth, above the lower alveolar canal.[25,28] Also, the focal and florid types affect the posterior area of the mandible, while the periapical group exhibits a predilection for the anterior mandible.[29] The findings of the current study support previous results.[26,30] In the present study, the mandible was more affected than the maxilla. Surprisingly, in addition to the periapical group, the most affected area in the florid group was the anterior region and it mostly involved 2 quadrants of the mandible.

There is no consensus among studies on the frequency of subgroups. In a retrospective study conducted in North and South America, the most common type reported was periapical OD.[30] Meanwhile, an international multicenter study from Africa reported that florid OD was the most common form.[31] In the present study, the most common types identified among 46 diagnosed cases of OD were focal and florid. This result may be related to the fact that florid OD is more symptomatic than other types. However, the groups also exhibited changes with respect to age. The florid group appeared at an older age (47.53 ±8.46 years) and the periapical group appeared at a younger age (36.23 ±8.97 years). In the middle-aged group, uniformly radiolucent density and the mixed stage were predominant, while in the group above the middle age, homogeneous radiopaque masses with calcification were most commonly observed. This general result is in accordance with previous radiographic data.[32] Such increased radiopacity indicates a greater degree of avascular mineralized tissue formation.

Relationships with anatomic structures in the current study were similar to the previously reported ones.[33] In this study, OD lesions affected both the buccal and lingual cortical bone ($n = 49$), the mandibular canal ($n = 19$), the anterior mandibular canal ($n = 5$), and the mental foramen ($n = 2$). In addition, the incisive foramen ($n = 2$), the maxillary sinus ($n = 2$) and the nasal fossa ($n = 2$) were involved. Generally, the lesions were characterized by well-defined partially corticated, hypodense images of an irregular shape with mixed density. The presence of hypodense capsules can facilitate OD diagnosis. In the present study, they were mostly detected in the periapical and florid groups. However, in 37.5% of lesions in the focal group, hypodense capsules were partially or completely absent. Therefore, care should be taken when diagnosing focal OD.

Panoramic radiography is an easily accessible and routinely used imaging method in clinical dentistry, but it is a two-dimensional (2D) modality with disadvantages such as superposition and magnification. Furthermore, it is insufficient to determine the radiological characteristics of OD lesions in a millimeter-scale examination of anatomical structures, e.g., the periodontal ligament space, lamina dura and the cortical bone. Cone-beam computed tomography is a frequently preferred imaging method in the diagnosis of maxillofacial pathologies due to its 3D evaluation feature, a lower radiation dose, and sub-millimeter image resolution as compared to computed tomography (CT).[34] In the present study, the lesion volumes were determined using 3D images, and cortical bone changes were compared with volume measurements for the first time.

The anatomical structure most affected was the cortical bone, especially the buccal cortex. The thinning of the cortical bone was the most common type of damage observed. However, when the lesion volume increased, the bone damage changed from intact to perforation, and when the total calcified volume was evaluated, it was significantly lower in the periapical group. When age-related changes were assessed, calcification was detected earlier in the periapical group than in the other groups. The amount of calcified tissue in the lesion increased with time and reached stage 3. Differences in the amount of calcified tissue between the groups may result from age differences.

With regard to the 2D measurements taken in previous studies, the lesions show greater growth in the mesiodistal direction than in other planes.[3,28] Additionally, in this study, mesiodistal directionality and greater growth in the superoinferior direction were also observed, which may indicate that the lesions do not display tumoral growth and expand to the cancellous bone.

The discontinuity of lamina dura was observed in 83.0% of cases, and an irregular periodontal ligament space was found in 67.0%. In total, only 5.7% of cases involved tooth displacement. Similar results were obtained in another 3D study, where the authors emphasized that the persistence of pulp vitality, along with the absence of tooth mobility, supported the outcome of the harmonic disorder between periodontal structures and OD lesions.[3] It also supported the theory of the origin of the lesion from the periodontal ligament tissue.[3] On the contrary, in a previous 2D imaging study, 77.6% of lamina dura was intact and periodontal ligament space was normal in 92.1% of cases.[30] However, this may be related to the limitations of 2D imaging.

In this study, only 1 patient in the florid group exhibited root resorption. Similarly, few studies have reported root resorption associated with OD,[15,30] whereas De Oliveira Kato et al. reported a significant number of cases demonstrating root resorption.[3] Root resorption is considered an indicator of damage severity.[35] Endodontic, orthodontic and periodontal factors that may cause a root change must be eliminated.

Limitations

The limitations of this study are related to its retrospective cross-sectional design and the evaluation of a limited number of cases. Further information on the radiological features of OD lesions is required by expanding the study with more cases.

Conclusions

In conclusion, OD was more prevalent in female patients, and the anterior mandible was the most affected bone in all types of OD. Osseous dysplasia lesions mostly affected anatomical structures by thinning the buccal cortical bone. Also, in 3D evaluation, the volume of the lesions increased, and the damage to the surrounding cortical bone also increased. The 3D assessment of frequently detected OD lesions and their clinical morphological features is extremely important for monitoring lesion development, distinguishing the lesions from other pathologies and observing their relationships with the surrounding anatomical structures.

Ethics approval and consent to participate

The research was approved by the ethics committee at the Faculty of Medicine of the Recep Tayyip Erdoğan University, Rize, Turkey, approved this research (reference number 2020/189). All patients provided written informed consent.

Data availability

The datasets generated and/or analyzed during the current study are available from the corresponding author on reasonable request.

Consent for publication

Not applicable.

ORCID iDs

Dilara Nil Günaçar https://orcid.org/0000-0002-9607-6362
Taha Emre Köse https://orcid.org/0000-0003-3601-0393
Banu Arıcıoğlu https://orcid.org/0000-0002-1124-1905
Erhan Çene https://orcid.org/0000-0001-5336-6004

References

1. Kuc I, Peters E, Pan J. Comparison of clinical and histologic diagnoses in periapical lesions. *Oral Surg Oral Med Oral Pathol Oral Radiol Endod*. 2000;89(3):333–337. doi:10.1016/s1079-2104(00)70098-9
2. De Oliveira Kato CdNA, Almeida de Arruda JA, Mendes PA, et al. Infected cemento-osseous dysplasia: Analysis of 66 cases and literature review. *Head Neck Pathol*. 2020;14(1):173–182. doi:10.1007/s12105-019-01037-x
3. De Oliveira Kato CdNA, Barra SG, Pimenta Amaral TM, et al. Cone-beam computed tomography analysis of cemento-osseous dysplasia-induced changes in adjacent structures in a Brazilian population. *Clin Oral Investig*. 2020;24(8):2899–2908. doi:10.1007/s00784-019-03154-x

4. Speight PM, Takata T. New tumour entities in the 4th edition of the World Health Organization Classification of Head and Neck tumours: Odontogenic and maxillofacial bone tumours. *Virchows Arch*. 2018;472(3):331–339. doi:10.1007/s00428-017-2182-3
5. Neville BW, Damm DD, Allen CM, Bouquot JE. *Oral and Maxillofacial Pathology*. 3rd ed. St. Louis, MO: Saunders Elsevier; 2009:640–645.
6. Fenerty S, Shaw W, Verma R, et al. Florid cemento-osseous dysplasia: Review of an uncommon fibro-osseous lesion of the jaw with important clinical implications. *Skeletal Radiol*. 2017;46(5):581–590. doi:10.1007/s00256-017-2590-0
7. MacDonald-Jankowski DS. Fibro-osseous lesions of the face and jaws. *Clin Radiol*. 2004;59(1):11–25. doi:10.1016/j.crad.2003.07.003
8. Rossbach HC, Letson D, Lacson A, Ruas E, Salazar P. Familial gigantiform cementoma with brittle bone disease, pathologic fractures, and osteosarcoma: A possible explanation of an ancient mystery. *Pediatr Blood Cancer*. 2005;44(4):390–396. doi:10.1002/pbc.20253
9. Şakar O, Aren G, Mumcu Z, Ünalan F, Aksakallı N, Tolgay CG. Familial gigantiform cementoma with Ehlers–Danlos syndrome: A report of 2 cases. *J Adv Prosthodont*. 2015;7(2):178–182. doi:10.4047/jap.2015.7.2.178
10. Pereira Cavalcanti PH, Leandro Nascimento EH, Dos Anjos Pontual ML, et al. Cemento-osseous dysplasias: Imaging features based on cone beam computed tomography scans. *Braz Dent J*. 2018;29(1):99–104. doi:10.1590/0103-6440201801621
11. Alsufyani NA, Lam EW. Cemento-osseous dysplasia of the jaw bones: Key radiographic features. *Dentomaxillofac Radiol*. 2011;40(3):141–146. doi:10.1259/dmfr/58488265
12. Di Primio G. Benign spotted bones: A diagnostic dilemma. *CMAJ*. 2011;183(4):456–459. doi:10.1503/cmaj.091740
13. Yonetsu K, Yuasa K, Kanda S. Idiopathic osteosclerosis of the jaws: Panoramic radiographic and computed tomographic findings. *Oral Surg Oral Med Oral Pathol Oral Radiol Endod*. 1997;83(4):517–521. doi:10.1016/s1079-2104(97)90156-6
14. Michetti J, Maret D, Mallet JP, Diemer F. Validation of cone beam computed tomography as a tool to explore root canal anatomy. *J Endod*. 2010;36(7):1187–1190. doi:10.1016/j.joen.2010.03.029
15. Gumru B, Akkitap MP, Deveci S, Idman E. A retrospective cone beam computed tomography analysis of cemento-osseous dysplasia. *J Dent Sci*. 2021;16(4):1154–1161. doi:10.1016/j.jds.2021.03.009
16. Köse TE, Köse OD, Karabas HC, Erdem TL, Ozcan I. Findings of florid cemento-osseous dysplasia: A report of three cases. *J Oral Maxillofac Res*. 2014;4(4):e4. doi:10.5037/jomr.2013.4404
17. Seigel DG, Podgor MJ, Remaley NA. Acceptable values of kappa for comparison of two groups. *Am J Epidemiol*. 1992;135(5):571–578. doi:10.1093/oxfordjournals.aje.a116324
18. Faul F, Erdfelder E, Lang AG, Buchner A. G*Power 3: A flexible statistical power analysis program for the social, behavioral, and biomedical sciences. *Behav Res Methods*. 2007;39(2):175–191. doi:10.3758/bf03193146
19. Ahmad M, Gaalaas L. Fibro-osseous and other lesions of bone in the jaws. *Radiol Clin North Am*. 2018;56(1):91–104. doi:10.1016/j.rcl.2017.08.007
20. Delai D, Bernardi A, Felippe GS, Da Silveira Teixeira C, Felippe WT, Santos Felippe MC. Florid cemento-osseous dysplasia: A case of misdiagnosis. *J Endod*. 2015;41(11):1923–1926. doi:10.1016/j.joen.2015.08.016
21. DiFiore PM, Bowen SE. Cemento-osseous dysplasia in African-American men: A report of two clinical cases. *J Tenn Dent Assoc*. 2010;90(4):26–28. PMID:21755799.
22. Senia ES, Sarao MS. Periapical cemento-osseous dysplasia: A case report with twelve-year follow-up and review of literature. *Int Endod J*. 2015;48(11):1086–1099. doi:10.1111/iej.12417
23. Su L, Weathers DR, Waldron CA. Distinguishing features of focal cemento-osseous dysplasia and cemento-ossifying fibromas. II. A clinical and radiologic spectrum of 316 cases. *Oral Surg Oral Med Oral Pathol Oral Radiol Endod*. 1997;84(5):540–549. doi:10.1016/s1079-2104(97)90271-7
24. Köklü HK, Cankal DA, Bozkaya S, Ergün G, Bar E. Florid cemento-osseous dysplasia: Report of a case documented with clinical, radiographic, biochemical and histological findings. *J Clin Exp Dent*. 2013;5(1):e58–e61. doi:10.4317/jced.50854
25. Toledano-Serrabona J, Núñez-Urrutia S, Vegas-Bustamante E, Sánchez-Torres A, Gay-Escoda C. Florid cemento-osseous dysplasia: Report of 2 cases. *J Clin Exp Dent*. 2018;10(11):e1145–e1148. doi:10.4317/jced.55288
26. Santos Netto JdN, Cerri JM, Aguiar Miranda AM, Pires FR. Benign fibro-osseous lesions: Clinicopathologic features from 143 cases diagnosed in an oral diagnosis setting. *Oral Surg Oral Med Oral Pathol Oral Radiol*. 2013;115(5):e56–e65. doi:10.1016/j.oooo.2012.05.022
27. Olgac V, Sinanoglu A, Selvi F, Soluk-Tekkesin M. A clinicopathologic analysis of 135 cases of cemento-osseous dysplasia: To operate or not to operate? *J Stomatol Oral Maxillofac Surg*. 2021;122(3):278–282. doi:10.1016/j.jormas.2020.06.002
28. Aiuto R, Gucciardino F, Rapetti R, Siervo S, Bianch AE. Management of symptomatic florid cemento-osseous dysplasia: Literature review and a case report. *J Clin Exp Dent*. 2018;10(3):e291–e295. doi:10.4317/jced.54577
29. Macdonald-Jankowski DS. Focal cemento-osseous dysplasia: A systematic review. *Dentomaxillofac Radiol*. 2008;37(6):350–360. doi:10.1259/dmfr/31641295
30. Alsufyani NA, Lam EW. Osseous (cemento-osseous) dysplasia of the jaws: Clinical and radiographic analysis. *J Can Dent Assoc*. 2011;77:b70. PMID:21683027.
31. Pereira DL, Pires FR, Lopes MA, et al. Clinical, demographic, and radiographic analysis of 82 patients affected by florid osseous dysplasia: An international collaborative study. *Oral Surg Oral Med Oral Pathol Oral Radiol*. 2016;122(2):250–257. doi:10.1016/j.oooo.2016.04.013
32. Kato CN, Barra SG, Pereira MJ, et al. Mandibular radiomorphometric parameters of women with cemento-osseous dysplasia. *Dentomaxillofac Radiol*. 2020;49(4):20190359. doi:10.1259/dmfr.20190359
33. De Moura RR, Campos Coelho AV, Balbino VdQ, Crovella S, Cavalcanti Brandão LA. Meta-analysis of Brazilian genetic admixture and comparison with other Latin America countries. *Am J Hum Biol*. 2015;27(5):674–680. doi:10.1002/ajhb.22714
34. Kursun S, Hakan KM, Bengi O, Nihat A. Use of cone beam computed tomography to determine the accuracy of panoramic radiological markers: A pilot study. *J Dent Sci*. 2015;10(2):167–171. doi:10.1016/j.jds.2013.04.003
35. Darcey J, Qualtrough A. Resorption: Part 1. Pathology, classification and aetiology. *Br Dent J*. 2013;214(9):439–451. doi:10.1038/sj.bdj.2013.431